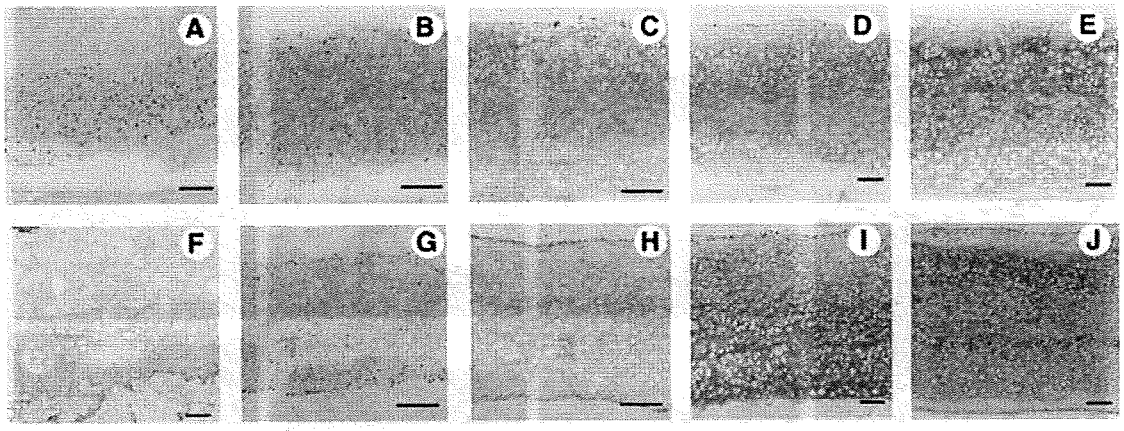

FIG. 4. Immunohistochemistry of paraffin sections of chondrocyte plate formed after 7 days of primary SC (A). Sections of chondrocyte plate formed after 1 week (B), 2 weeks (C), 3 weeks (D), and 5 weeks (E) of SC. Sections of chondrocyte plate formed after 1 week (G), 2 weeks (H), 3 weeks (I), and 5 weeks (J) of rotational culture. Normal articular cartilage (4-week-old Japanese white rabbits) (F). Chondrocyte plate at week 5 of SC was strongly stained with type II collagen antibody (E). Chondrocyte plates at weeks 3 and 5 of RC were strongly stained with type II collagen antibody (I, J). Magnifications of objective lens, ×4. Scale bar = 100 μm. Color images available online at www.liebertonline.com/ten.

Thickness and tensile properties

In both the RC and SC groups, thickness increased rapidly from 1 to 2 weeks. The rate of increase in thickness in the RC group was maintained up to week 5 of culture, whereas in the SC group, it tended to decrease (Fig. 6).

Young's modulus tended to increase after each week of culture in the RC group when compared with the SC group. In the SC group, there was no significant increase by 3 weeks, but the increase was significant at 5 weeks. In the RC group, there was no significant increase at 2 weeks, but the increase was significant by 3 weeks (Fig. 7).

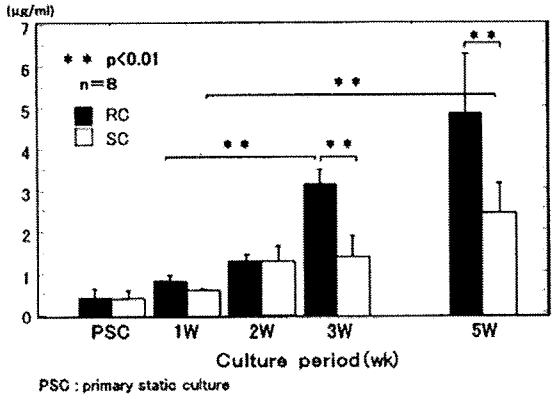

FIG. 5. Collagen type II expression of the chondrocyte plate during 5 weeks of culture was measured by enzyme-linked immunosorbent assay. Collagen type II expression was increased at 3 weeks of RC and at 5 weeks of SC. PSC, primary SC.

Time-resolved laser-induced fluorescence spectroscopy

Changes were evaluated in peak wavelength at each week of culture of the TEC. In the SC group, there was no significant change at 3 weeks, but there was a significant change at 5 weeks. In the RC group, there was no significant change at 2 weeks, but at 3 weeks, there was a significant change (Fig. 8).

Discussion

The increasingly common clinical application of regenerative medicine has become a reality with advances in technology. Therefore, noninvasive methods are essential for real-time monitoring of tissue constructs, from the time of production to before, during, and after implantation. In our study, scaffold-free TEC was produced by simple RC, based

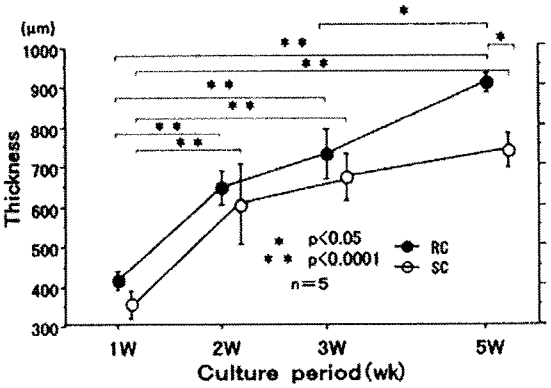

FIG. 6. Time changes in thickness of the chondrocyte plate during 5-week RC. Thickness of the cartilage plate was measured using a digital micrometer.

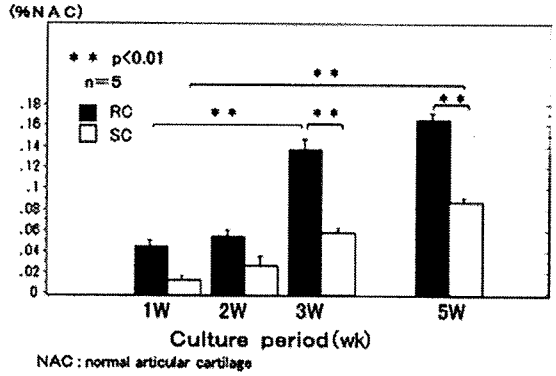

FIG. 7. Time changes in Young's modulus of the chondrocyte plate during 5 weeks of culture. Young's modulus of the chondrocyte plate was increased at 3 weeks of RC and at 5 weeks of SC. NAC, normal articular cartilage.

on the principle that chondrocytes dedifferentiated in high-density cell culture (due to cell-cell adhesions and interaction) will redifferentiate, and that mechanical stress is required for chondrocyte redifferentiation. Furukawa *et al.* and Nagai *et al.* have reported the usefulness of RC based on assays for proteoglycans, DNA, collagen, and collagen type I and II mRNA, and based on physical characteristics (tensile testing).[13–16] In our study, ELISA quantification of type II collagen also showed that RC significantly increased type II collagen production. These results were confirmed by fluorescence spectroscopy. Articular cartilage is hyaline cartilage, a tissue composed of about 2% chondrocytes and abundant ECM. ECM is composed of about 70% water, 20% collagen, and 10% proteoglycans or cell components. In addition, of the collagen that comprises 20% of hyaline cartilage, 80–90% is type II collagen. In other words, most articular cartilage tissue is type II collagen. The autofluorescence within the tissue is caused by collagen and coenzyme NAD(P)H in cell components. Thus, fluorescence emissions from cartilage are mostly due to type II collagen. Type II collagen has attracted interest as an autofluorescent substance and for its important role in the viscoelastic properties of chondrocytes.[9,18] In our study, 5-week culture and serial fluorescence spectroscopy were performed. Changes in quantitative results and fluorescence peak wavelength of the TEC were compared. Type II collagen was significantly increased in the RC group at 3 weeks, and in the SC group at 5 weeks. Fluorescence peak wavelength also changed significantly in the RC group at 3 weeks (shifted to shorter wavelength), and in the SC group at 5 weeks. These findings indicate that in the RC group, type II collagen production was significantly increased as compared to the SC group. This occurred from weeks 2 to 3 of culture, and was easily discerned by changes in peak wavelength. Physical properties were also evaluated. Tensile strength of tissue generally correlated with collagen content, and compression strength generally correlated with proteoglycan content.[18,19] In this study, we measured tensile strength of the TEC. The results correlated both with changes in type II collagen content and changes in peak wavelength. Further, correlation analysis regarding type II collagen content, peak wavelength, and Young's modulus revealed significant correlations among all parameters. Peak wavelength reflected the type II collagen content of the sample, and it was clarified that it is possible to quantitatively evaluate the constituent representing the largest component ratio (Fig. 9). These results suggest the possibility of quantitatively evaluating other autofluorescent materials through analysis of the substance-specific fluorescence wavelength.

These changes also correlated with the immunostaining results for type II collagen. The peak wavelength data obtained by TR-LIFS were thought to reflect autofluorescence at the highest composition ratios among the sample autofluorescence substances. Tensile strength increased with culture duration (weeks); this increase corresponds to a rise in the type II collagen composition ratio.

The reason for the considerably lower strength, as compared to normal cartilage, is because tensile strength is influenced not only by type 2 collagen content but also by fiber orientation, tissue proteoglycan content, and cell density. In our study samples, Nagai, from our research group, measured PG content. This was markedly higher in 3-week cultures than in normal cartilage.[15] In addition, our study sample considerably has a higher cell density than has a normal articular cartilage tissue. Based on our results, changes in peak wavelength on fluorescence spectroscopy can be used to validate a tissue engineering cartilage culturing process. In 2004, Ashjian *et al.* measured autofluorescence of osteoinduced PLA cells and performed a detailed analysis.[16] Spectroscopy of PLA cells not osteoinduced showed broad emission with a peak wavelength of 420–430 nm. This wavelength corresponded to the spectrum of skin-derived type I collagen and placenta-derived types IV and V collagen. Their results showed characteristics similar to the fluorescence spectrum of juvenile rabbit chondrocytes immediately after isolation. Although they reported no significant changes, spectroscopy of the osteoinduced PLA cells showed that the peak wavelength shifted toward 450 nm at 3, 5, and 7 weeks. This shift in peak wavelength was thought to indirectly represent differentiation of PLA cells to bone. They also analyzed the decay time using TR-LIFS and reported that spectroscopy

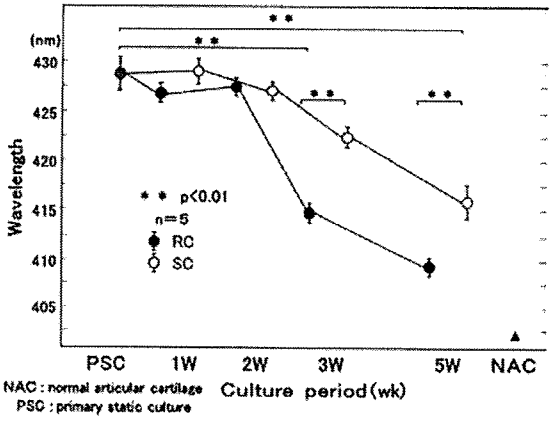

FIG. 8. Time changes in peak wavelength of the chondrocyte plate during 5-week RC. Peak wavelength of the chondrocyte plate decreased at 3 weeks of RC and at 5 weeks of SC.

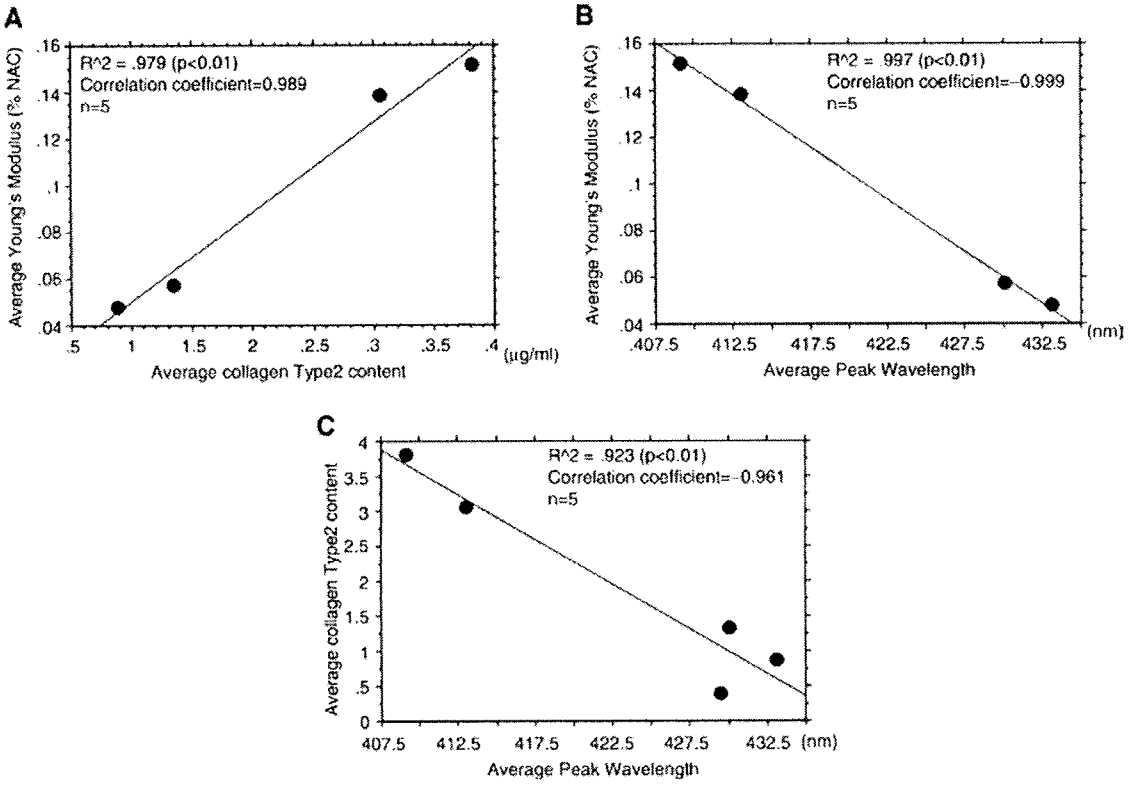

FIG. 9. (A) Correlation of average Young's modulus to average collagen type 2 content. (B) Correlation of average Young's modulus to average peak wavelength. (C) Correlation of average collagen type 2 content to average collagen peak wavelength.

of the osteoinduced PLA cells was characteristic for mainly type I collagen, and they stated that based on decay characteristics alone, collagen expression could be monitored. However, our study results suggest that when there is a specific tissue composition like hyaline cartilage, the changes in peak wavelength permit monitoring of type II collagen production. In addition, the serial changes in the fluorescence spectrum of osteoinduced PLA cells are similar to changes in the fluorescence spectrum associated with passages of juvenile rabbit chondrocytes in monolayer culture. Chondrocytes with a peak wavelength of 420–430 nm just after isolation that maintained differentiation produced collagen and formed TEC. The fluorescence peak wavelength shifted to 400 nm during culture, whereas the fluorescence peak wavelength of juvenile rabbit chondrocytes in monolayer culture shifted to 440–450 nm as the number passages increased (data not shown). At the excitation wavelength of NAD(P)H (290–350 nm), the fluorescence wavelength is 440–464 nm.[20–22] In addition, a decrease in collagen fluorescence and marked increase in NAD(P)H fluorescence have been reported with increased cell number and tissue dysplasia.[20,23] Therefore, the shift toward shorter wavelengths and the shift toward longer wavelengths represent collagen production when cell differentiation is maintained, and a decreased ability to produce collagen during cell dedifferentiation, respectively. When evaluating known tissue characteristics, tissue autofluorescence can be identified by peak wavelengths alone. However, when detecting autofluorescence in unknown tissues, as noted, a shift toward a shorter peak wavelength does not necessarily indicate chondrogenesis, and a shift toward a longer peak wavelength does not necessarily indicate osteogenesis. For example, type I collagen from bovine Achilles tendon (peak 380 nm, decay time 5.2 ± 0.2 ns) and calf skin (peak 420 nm, decay time 1.05 ± 0.1 ns) have markedly different peak wavelengths and decay times.[25] If the peak wavelength of a tissue at the measurement start time is, for example, 390 nm, whether this is a shift to a longer wavelength representing chondrogenesis or osteogenesis cannot be assessed based on peak wavelength alone. In this case, assessing the decay time of each wavelength using TR-LIFS will help to distinguish chondrogenesis from osteogenesis based on lengthening or shortening. In our study, although the data are not shown, decay time was calculated, and characteristic lengthening or shortening of decay times at each wavelength was found based on culture duration (weeks) and culture method. For example, our data showed that the decay time of the type II collagen peak wavelength at 402 nm, with the initial SC (PSC1W) as a reference, shortened at week 1, was significantly prolonged at week 2, and remained the same at week 3. This finding suggests a process by which dediffer- ◀AU5

entiated monolayer cultured chondrocytes redifferentiate in a 3D culture, and to identify phenotypic modulations at a specific time, decay time must also be assessed. The above parameters must be comprehensively considered. When peak wavelength alone is used as a parameter, it can only be confirmed by the variability pattern. Thus, deviations from this variability pattern suggest a material that may not be ideal for regenerative tissue.

In our study, changes in fluorescence peak wavelength of the TEC were correlated with changes in type II collagen content. This demonstrates that monitoring changes in peak wavelength enables noninvasive evaluation of cartilage formation. This method of analysis may be useful in the advancing field of cartilage regenerative medicine.

Acknowledgments

We thank Ms. Aya Saito, Ms. Mami Kokubo, and Ms.Tomoko Nakai for their expert technical assistance. This work was partially supported by New Energy and Industrial Technology Development Organization and Japan Foundation for Aging and Health.

AU6 ▶ ### Disclosure Statement

No competing financial interests exist.

References

1. Ishihara, M., Sato, M., Sato, S., Kikuchi, T., Fujikawa, K., and Kikuchi, M. Viscoelastic characterization of biological tissue by photoacoustic measurement. Jpn J Appl Phys **42,** 556, 2003.
2. Ishihara, M., Sato, M., Sato, S., Kikuchi, T., Fujikawa, K., and Kikuchi, M. Biomechanical characterization of tissue-engineered cartilages by photoacoustic measurement. SPIE Proc **4961,** 221, 2003.
3. Ishihara, M., Sato, M., Sato, S., Kikuchi, T., Mochida, J., and Kikuchi, M. Usefulness of photoacoustic measurements for evaluation of biomechanical properties of tissue-engineered
AU7 ▶ cartilage Tissue Eng 11, 2005.
4. Ishihara, M., Sato, M., Kaneshiro, N., Mitani, G., Sato, S., Mochida, J., and Kikuchi, M. Development of a diagnostic system for osteoarthritis using a photoacoustic measurement
AU7 ▶ method. Lasers Surg Med 38, 2006.
5. Ishihara, M., Sato, M., Kaneshiro, N., Mitani, G., Sato, S., Ishihara, M., Mochida, J., and Kikuchi, M. Development of a noninvasive multifunctional measurement method using nanosecond pulsed laser for evaluation of regenerative medicine for articular cartilage. SPIE Proc **6084,** 30, 2006.
6. de Veld, D.C.G., Witjes, M.J.H., van der Wal, J.E., Sterenborg, H.J.C.M., and Roodenburg, J.L.N. The status of *in vivo* autofluorescence spectroscopy and imaging for oral oncology. Oral Oncol **41,** 117, 2005.
7. Ashjian, P., Elbarbary, A., Zuk, P., DeUgarte, D.A., Benhaim,
AU8 ▶ P., and Hedrick, M.H. Tissue Eng **10,** 411, 2004.
8. Georgakoudi, I., Jacobson, B.C., Muller, M.G., Sheets, E.E., Badizadegan, K., Carr-Locke, D.L., Crum, C.P., Boone, C.W., Dasari, R.R., Van Dam, J., and Feld, M.S. NAD(P)H and collagen as *in vivo* quantitative fluorescent biomarkers of epithelial precancerous changes. Cancer Res **62,** 682, 2002.
9. Ramanujam, N. Fluorescence spectroscopy *in vivo*. In: Meyers, R.A., ed. Encyclopedia of Analytical Chemistry. Chichester, UK: John Wiley and Sons Ltd., 2000, pp. 20–56.
10. Miller, E.J., and Gay, S. The collagens: an overview and update. Methods Enzymol **144,** 3, 1987.
11. Fiorotti, R.C., Nicola, J.H., and Nicola, E.M.D. Native Fluorescence of oral cavity structures: an experimental study in dogs. Photomed Laser Surg **24,** 22, 2006.
12. Marcu, L., Cohen, D., Maarek, J.M.I., and Grundfest, W.S. Characterization of type I, II, III, IV, and V collagens by time-resolved laser-induced fluorescence spectroscopy. SPIE **3917,** 93, 2000.
13. Furukawa, K.S., Suenaga, H., Toita, K., Numata, A., Tanaka, J., Ushida, T., Sakai, Y., and Tateishi, T. Rapid and large-scale formation of chondrocyte aggregates by rotating culture. Cell Transplant **12,** 475, 2003.
14. Furukawa, K.S., Imura, K., Tateishi, T., and Ushida, T. Scaffold-free cartilage by rotating culture for tissue engineering. J Biotechnol **133,** 134, 2008.
15. Nagai, T., Furukawa, K.S., Sato, M., Ushida, T., and Mochida, J. Characteristics of a scaffold-free articular chondrocyte plate grown in rotating culture. Tissue Eng 14, 2008. ◀ AU7
16. Nagai, T., Sato, M., Furukawa, K.S., Kutsuna, T., Ohta, N., Ushida, T., and Mochida, J. Optimization of allograft implantation using scaffold-free chondrocyte plates. Tissue Eng 14, 2008. ◀ AU7
17. Mendler, M., Eich-Bender, S.G., Vaughan, L., Winterhalter, K.H., and Bruckner, P. Cartilage contains mixed fibrils of collagen type II, IX, and XI. J Cell Biol **108,** 191, 1989.
18. Gemmiti, C.V., and Guldberg, R.E. Fluid flow increases type II collagen deposition and tensile mechanical properties in bioreactor-grown tissue-engineered cartilage. Tissue Eng **12,** 469, 2006.
19. Poole, A.R., Kojima, T., Yasuda, T., Mwale, F., Kobayashi, M., and Laverty, S. Composition and structure of articular cartilage: a template for tissue repair. Clin Orthop **391,** S26, 2001.
20. Lakowicz, J.R. Principles of Fluorescence Spectroscopy. New York: Plenum Press, 1999.
21. Pradhan, A., Pal, P., Durocher, G., Villeneuve, L., Balassy, A., Babai, F., Gaboury, L., and Blanchard, L. Steady state and time resolved fluorescence properties of metastatic and non-metastatic malignant cells from different species. J Photochem Photobiol B Biol **3,** 101, 1995.
22. Glassman, W.S., Steinberg, M., and Alfano, R.R. Time Resolved and Steady State Fluorescence Spectroscopy from (1999). ◀ AU9
23. Mayevsky, A., and Chance, B. Intracellular oxidation-reduction state measured *in situ* by a multichannel fiber-optic surface fluorometer. Science **217,** 537, 1982.

Address correspondence to:
Masato Sato, M.D., Ph.D.
Department of Orthopaedic Surgery
Surgical Science
Tokai University School of Medicine
143 Shimokasuya, Isehara
Kanagawa 259-1193
Japan

E-mail: sato-m@is.icc.u-tokai.ac.jp

Received: January 6, 2009
Accepted: July 9, 2009
Online Publication Date:

In: Bioengineering: Principles, Methodologies and Applications ISBN: 978-1-60741-762-0
Editor: Audric Garcia and Ciel Durand

Chapter 7

DEVELOPMENT OF A DIAGNOSTIC SYSTEM FOR OSTEOARTHRITIS USING A PHOTOACOUSTIC MEASUREMENT METHOD AND TIME-RESOLVED AUTO-FLUORESCENCE

Masato Sato [1*], ***Miya Ishihara*** [1,2], ***Genya Mitani*** [1], ***Toshiharu Kutsuna*** [1], ***Jeong Ik Lee*** [1], ***Makoto Kikuchi*** [2], ***Joji Mochida*** [1]

[1] Department of Orthopaedic Surgery, Surgical Science, Tokai University School of Medicine, 143 Shimokasuya, Isehara, Kanagawa, 259-1193 Japan.
[2] Department of Medical Engineering, National Defense Medical College, 3-2 Namiki, Tokorozawa, Saitama, 359-8513 Japan.

Key words: Diagnostic system • Laser • Osteoarthritis • Photoacoustic measurement • Tissue-engineered cartilage

ABSTRACT

We have developed new methods to measure some essential properties of cartilage: a photoacoustic measurement method and time-resolved fluorescence spectroscopy. These can be used to evaluate the outcomes of tissue-engineered cartilage, regenerated articular cartilage tissue after surgery, and the degenerated cartilage of osteoarthritis patients. A nanosecond-pulsed laser, which is completely noninvasive, is focused onto the target cartilage and induces a photoacoustic wave, which will propagate with attenuation, which is affected by the viscoelasticity of the surrounding cartilage. The decay time during which the amplitude of the photoacoustic wave is reduced by a factor of 1/e is the key numerical value used to characterize and evaluate the viscoelasticity and rheological

* Corresponding author:
Masato Sato, MD., PhD., Associate Professor and Research Director, Department of Orthopaedic Surgery, Surgical Science, Tokai University School of Medicine 143 Shimokasuya, Isehara, Kanagawa, 259-1193 Japan. Email: sato-m@is.icc.u-tokai.ac.jp, TEL: +81-463-93-1121 (ext 2320), FAX: + 81-463-96-4404

behavior of the cartilage. In this study, we also investigated whether pulsed laser irradiation and the measurement of excited autofluorescence allow us to noninvasively evaluate tissue characters in real time. Our findings show that time-resolved laser-induced fluorescence spectroscopy is useful for evaluating tissue-engineered cartilage. This measurement system, predicated on the interactions between optics and living organs, is a suitable methodology for diagnosis during arthroscopy, because it allows the quantitative and multidirectional evaluation of the original function of the cartilage based on a variety of parameters.

INTRODUCTION

Osteoarthritis, which is thought to affect 24 million people in Japan [1], is not a direct threat to life. However, it both affects the activities of daily living and diminishes the quality of life of sufferers, so the associated human and social loss cannot be overestimated. The disease involves dysfunction caused by cartilage degeneration, but no objective evaluation methodologies based on the original function of the articular cartilage are currently available. Evaluations that are made to establish conservative therapies or the prognosis of surgery as a treatment for osteoarthritis are merely based on the patients' subjective symptoms or the degree of narrowing of the joint space on X-ray images. It is important to accurately measure and quantitatively evaluate the mechanical characteristics of the cartilage (viscosity, elasticity, and lubrication), and the tissue properties of the original articular cartilage to understand the pathological condition in detail and to judge the treatment effects. Therefore, the development of such an evaluation technology is required to facilitate a functional diagnosis of osteoarthritis (Table 1). If it is possible to do this noninvasively, then it should be possible to accurately understand the pathologies and plan and undertake treatments for locomotor apparatus diseases that accompany the degeneration of cartilage, such as osteoarthritis. It will also be useful as an objective evaluation methodology in clinical trials of new drugs, etc. It should thus be possible to better understand the pathological condition in detail and to make a prognosis based on a body of clinical data. This in turn will facilitate the careful planning of treatments according to pathological conditions of individual patients, improving their activities of daily living and enhancing the lives of many people. We propose the application of a unique measurement and evaluation methodology [2–15], which we have developed in vitro to noninvasively assess regenerating cartilage (tissue-engineered cartilage) and to diagnose cartilage degeneration.

SUPERIORITY OF THE USE OF LASER

The scattering, reflection, and increase in temperature attributable to absorption and the production of fluorescence and acoustic waves are regarded as the main effects when light or laser beams irradiate living organs to be measured (Figure 1) [12]. A noninvasive and selective diagnostic device that uses optics via an optical fiber has recently attracted attention. It is based on a technology that takes advantage of the interactions between optics and living organs. The use of these interactions makes possible the simultaneous collection of not only morphological information but also various physiological and biochemical data, so its

potential for use as a diagnostic device is greater than that of techniques based on a single type of information, such as ultrasonic waves. Bioinstrumentation and imaging with a laser beam, which have recently attracted attention, have features that facilitate the application of this technology to the medical field (Table 2). We focused on the interactions between living organs and optics, especially photoacoustic waves and fluorescence, measured a variety of parameters related to these interactions when induced by the same laser, and developed a system that allows the simultaneous evaluation of the mechanical characteristics and properties of tissue (Figure 2) [3–5].

Table 1. Comparison of the Evaluation Methods

The conventional methods to evaluate articular cartilage	To evaluate the essential functions of articular cartilage
1. Joint space loss (X ray diagnosis) 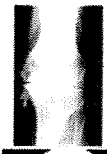	1. Viscoelastic characteristics → Photoacoustic measurement (Arthroscopic examination)
2. Appearance of the cartilage surface (Arthroscopic examination) 	2. Characterization of extracelluar matrix → Time-resolved autofluorescence spectroscopy (Arthroscopic examination)
3. Probing (Arthroscopic examination) 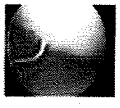	3. Lubricating behavior →difficult to measure *in vivo*
4. Histological assessment (Biopsy) 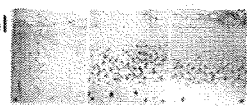	

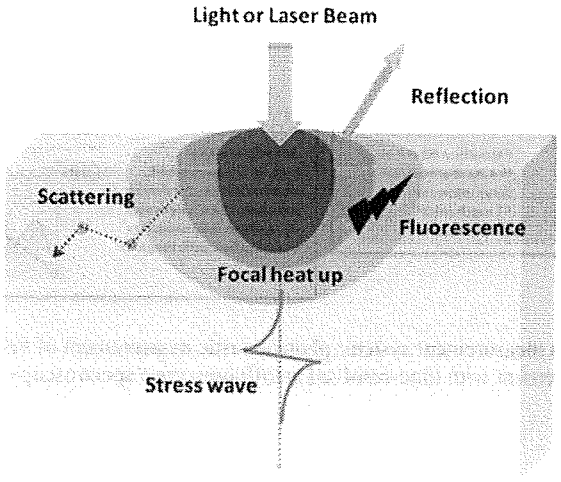

Figure 1. Mutual interaction between light and a living body

Table 2. Features of Laser for Medical Field

1. The safety and the non-invasiveness are guaranteed by choosing non-injurious wavelengths.
2. From the view point of mutual interaction between light and a living body, it is possible to analyze the properties of cells and tissues.
3. It can be applied broadly when measuring the targets, because the beams can be transferred through the thin fiber.
4. The advantages of easy portability are afforded by the downsized probes.
5. It is capable to give a simple and fast diagnosis by developing a new software program for analyses.

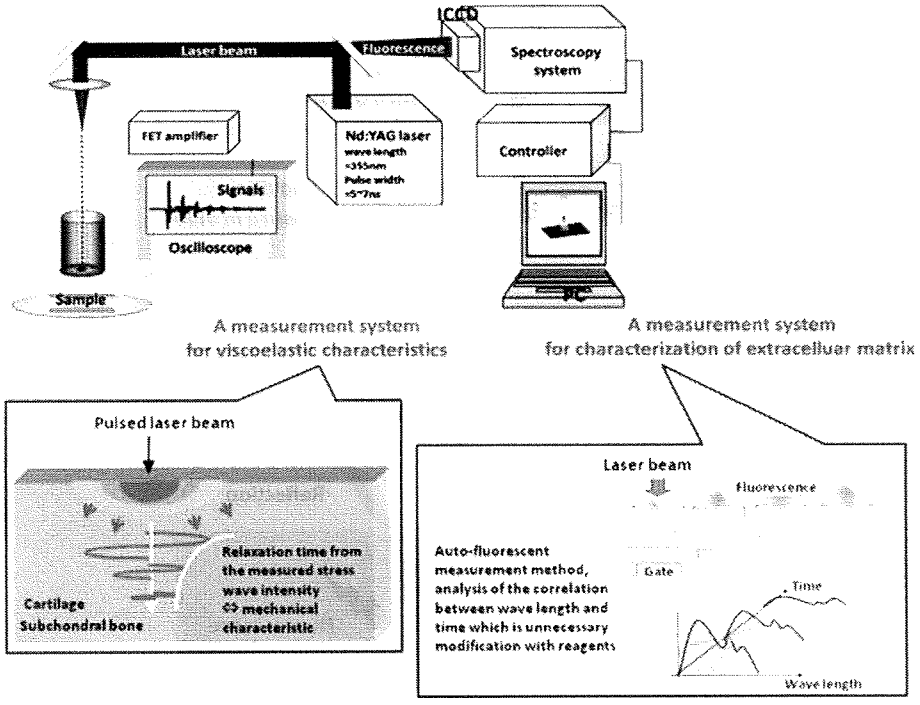

Figure 2. Simultaneous measurement system: photoacoustic measurement of viscoelastic characteristics and fluorescent measurement with time-resolved autofluorescence spectroscopy

EVALUATION OF MECHANICAL CHARACTERISTICS USING A PHOTOACOUSTIC METHOD

Tissue viscoelasticity affects the propagation and attenuation of the stress waves induced by pulsed laser irradiation [11]. The relaxation time of the stress wave, calculated as the time in which the amplitude of the stress wave decreases by a factor of 1/e, gives the intrinsic relaxation parameters (η/G) of the tissue, where η is the viscosity and G is the elasticity. We have proposed a basic principle whereby the mechanical characteristics of the tissue can be measured with photoacoustic parameters. In this measurement technique, the relaxation time of the stress that acts on a linear viscoelastic object (consisting of a spring and a dashpot) is related to the viscoelastic parameters of the object, and to the damping time of the stress waves that are generated by irradiation with a nanosecond pulse laser. The relaxation time is theoretically related to the viscous-to-elastic modulus rate [12]. The relaxation time (τ) is calculated using the Levenberg–Marquardt algorithm, a nonlinear least-squares method, as follows. When the stress wave intensity is attenuated only by its reflection at the boundaries and its relaxation during its transmission through viscoelastic materials, then the time course of the stress wave intensity is expressed by the following equation [2]:

$$I_\delta = I_0 \times R \times \exp(-t_\delta / \tau)$$

where Io is the intensity of the stress wave at t = 0, R is the product of reflectivity (the product of the internal reflectivity at the interface at both ends of the sample), t_δ is the time after laser irradiation, and τ is the decay time of the stress wave and corresponds to the ratio of viscosity to elasticity.

Because the optimum wavelength of the laser beam was unknown at the beginning of this study, we used an optical parametric oscillator (Spectra-Physics K.K., Tokyo, Japan) and set the oscillation wavelength within the range of 250–355 nm, with collagen and protein as the optical chromophore, and it was thus possible to measure the photoacoustic signals at any wavelength within this range [11]. The shorter wavelengths within this wavelength range can magnify the absorption by living organs, so it is possible to increase the peak value of the initiated photoacoustic waves and to set the initiation depth of the photoacoustic wave at a shallower level. However, in practical terms, a small, portable, and inexpensive excitation light source is desirable, so we devised a system in which the third harmonic frequency of a Q switch Nd:YAG laser (wavelength 355 nm, pulse width 5–6 ns; Excel Technology K.K., Japan) was used [13,14]. We developed a probe in which the optical output was introduced via a quartz glass optical fiber (core diameter 400 nm; Thorlabs Japan Inc., Japan), and the poly(polyvinylidene fluoride) copolymer (P[VdF/TrFE]) of a piezoelectric polymer film (Nishiki Trading Co., Ltd., Japan) was used to detect the photoacoustic waves [14]. In this system, the laser irradiation side and the measuring side were originally opposite, so it was only possible to evaluate permeable objects in vitro. However, with repeated trial and error, we developed an integrated optical fiber reflective probe that allowed measurements to be made in vivo, specifically during arthroscopy, by situating the probe at the center and placing the sensors peripherally around it in a circle (Figure 3).

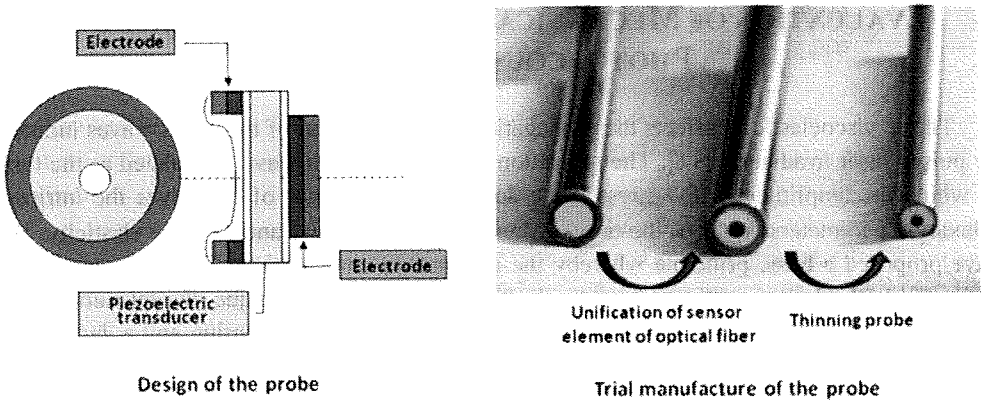

Figure 3. Development of the probe

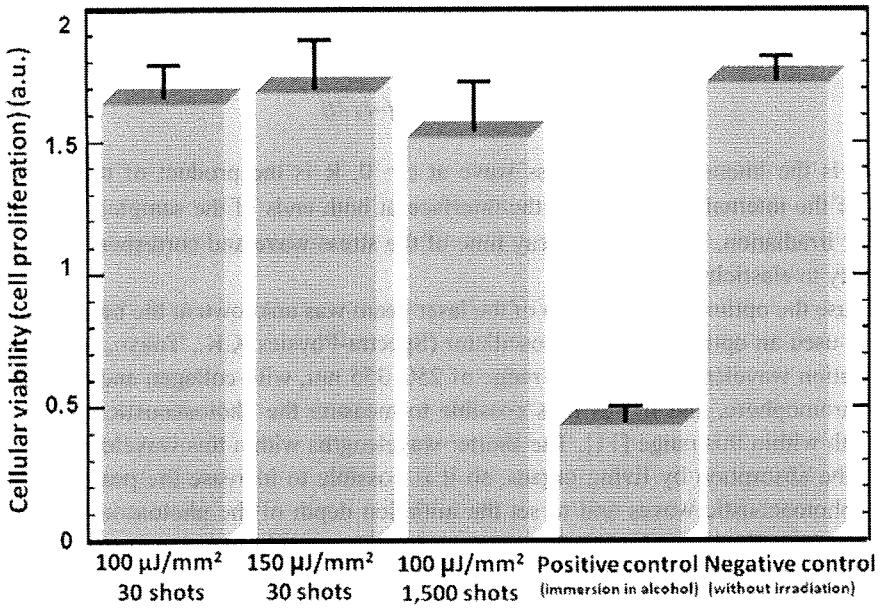

Figure 4. Effect of laser irradiation (energy per mm^2) on cell viability (cell proliferation)

SAFETY TEST

To assess the safety of the photoacoustic measurement method, we used a cell proliferative activity test in cultivated domestic rabbit chondrocytes and examined the effects on the chondrocytes of laser beam irradiation that induced photoacoustic signals. Because the irradiation conditions of the laser were based on the third harmonic generation of a Q switch

Nd:YAG laser with a wavelength of 355 nm, the following five groups were established and examined: (1) a group treated under clinically used radiation conditions (100 $\mu J/mm^2$, 30 shots); (2) a group treated under conditions in which the pulse energy was 1.5 times greater than that used clinically (150 $\mu J/mm^2$, 30 shots); (3) a group treated under conditions in which the number of pulse shots was 50 times higher than the number used clinically (150 $\mu J/mm^2$, 1,500 shots); (4) a positive control group to which 70% ethanol was added to kill the cells completely; and (5) a negative control with no laser irradiation. It should be noted that the pulse energy used to treat group (2) was the maximum output of this device. A WST-8 assay (Dojindo Laboratories, Japan) was used for the cell proliferative activity test. We applied the abovementioned conditions to cultivated cells sown in a 96-well plate and cultured at 37 °C under 5% CO_2, with all measurements made after 1 h. We confirmed that there were no significant differences between any laser-irradiated group and the nonirradiated group, so laser irradiation had no effect on cell proliferative activity (Figure 4) [14].

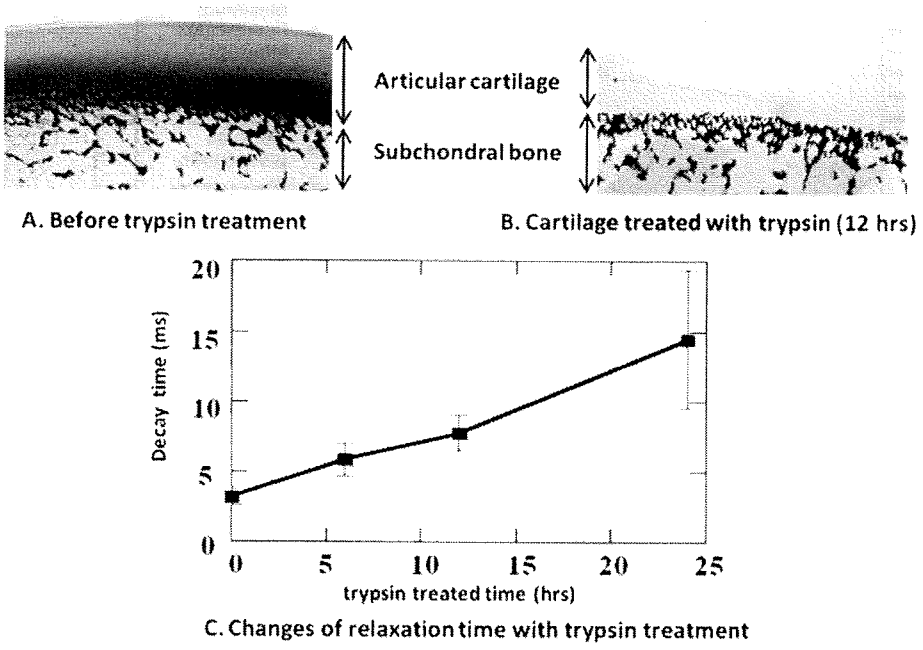

Figure 5. The photoacoustic evaluation of characteristic viscoelastic changes with cartilage degeneration

Evaluation of Degenerated Cartilage

To produce experimentally degenerated cartilage, we created cartilage with different degrees of degradation by extracting osteochondral plugs, with a diameter of 12 mm, from swine patellar cartilage and processing them with trypsin (trypsin–1 × EDTA; Gibco,

Invitrogen Corp., Carlsbad, Canada) to cause an outflow of proteoglycan, reflecting the changes in the mechanical characteristics of the tissue in vivo. The trypsin concentration was 1 mg/mL and it was applied for up to 24 h. We assessed the degenerated cartilage using the photoacoustic measurement method. After the measurements had been made, the samples were fixed in 10% formalin solution for histological study. The samples were sectioned to 4 μm thick slices for microscopic observation and stained with toluidine blue. Figure 5 shows the positive correlation between the decay time and the trypsinization time [14]. Specifically, the decay time increased as the trypsinization time increased. In other words, the viscosity increased and the elasticity decreased. Histologically, the stainability of the tissue with toluidine blue also decreased with trypsinization and the loss of proteoglycans, suggesting that it is possible to monitor the course of the tissue changes involved in cartilage degeneration using the photoacoustic measurement method.

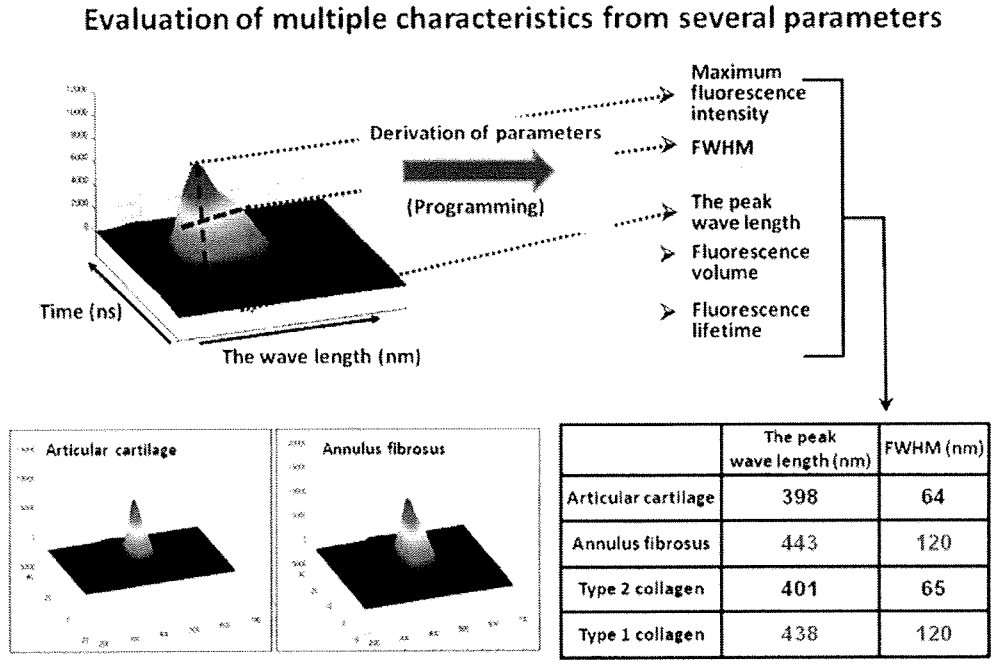

	The peak wave length (nm)	FWHM (nm)
Articular cartilage	398	64
Annulus fibrosus	443	120
Type 2 collagen	401	65
Type 1 collagen	438	120

Figure 6. Analyses with time-resolved autofluorescence spectroscopy

PROPERTY EVALUATION USING TIME-RESOLVED AUTOFLUORESCENCE SPECTROSCOPY

For time-resolved autofluorescence spectroscopy, we used the third harmonic generation of the Q switch Nd:YAG laser for the excitation light introduced via an optical fiber, in a manner similar to that used in the photoacoustic measurement method. We used a CCD

sensor with an image intensifier as the photodetector, while controlling the spectroscopic system that could be measured by a nanosecond order gate with a four-channel digital pulse generator. The fluorescence peak intensity, half bandwidth, peak wavelength, fluorescence volume, and fluorescence life were calculated as the measurement parameters. The articular cartilage of Japanese white domestic rabbits, the outer layer of the annulus fibrosus, and commercially available type I and type II collagen (powder; Ieda Chemical Co., Ltd., Japan) were used as the target samples. The articular cartilage exhibited a spectrum close to that of type II collagen, and the peak wavelengths and half bandwidths were also similar. Conversely, the outer layer of the annulus fibrosus exhibited a spectrum close to that of type I collagen, and the peak wavelengths and half bandwidths were also similar (Figure 6) [2,12]. This indicates that it is possible to measure the collagen composition of tissue, because collagen is an autofluorescent substance used in vivo in a noncontact manner. This is significant because the content ratio of type I to type II collagen is especially important in diagnosing the degree of cartilage degradation[16].

APPLICATION IN THE MEDICAL FIELD

Many elderly people who suffer from lifestyle-related diseases are also affected by osteoarthritis and are often unable to perform exercises that would normally be within their physical capacity because of joint pain and a limited range of motion. This is particularly serious in patients with diabetes, hyperlipidemia, or obesity, and their disease may be exacerbated because osteoarthritis reduces their ability to exercise, even when exercise therapy is available. In osteoarthritis, evaluating the prognosis of conservative therapy or the treatment effects after surgery often depends on the patient's subjective symptoms, so the pathological condition is not accurately understood. Surgical treatments, such as artificial joint replacement, are currently performed on patients in the terminal phase, whereas patients in the initial to middle phases are treated conservatively, often without any clear aims.

This study has demonstrated that it is possible to evaluate the mechanical characteristics and properties of articular cartilage simultaneously during arthroscopy using a noninvasive intense pulsed laser. We are now developing a device for this application by trial and error. If such a device is developed, an accurate measurement of the mechanical characteristics of the original function of the articular cartilage and the associated tissue properties will be possible during arthroscopy, and anyone could make such a quantitative functional evaluation. Therefore, it will be possible to accurately understand the pathological features of osteoarthritis and to carefully plan and undertake treatments. This technology could also quantitatively measure and evaluate mechanical characteristics and tissue properties simultaneously, to assess treatment effects, such as those of a variety of drugs, in addition to the conventional evaluation of clinical symptoms such as pain or inflammation around the joints. We believe that this methodology will be useful in the objective evaluation of articular cartilage in the clinical trials of new drugs, etc. This diagnostic system is a methodology used during arthroscopy, so it cannot be a completely noninvasive evaluation [15]. However, if quantitative data are collected during arthroscopy treatments, it will be possible to predict the effects of a variety of conservative therapies, based on the severity of cartilage degeneration. Therefore, it will be possible to carefully plan and undertake treatments on an individual

patient basis. Accordingly, we are certain that the development of this technology and practical diagnostic devices will improve the patients' activities of daily living and quality of life, and thus contribute to a healthy life expectancy.

CONCLUSION

1. A photoacoustic measurement method using a noninvasive nanosecond-pulsed laser allowed the evaluation of the mechanical characteristics of cartilage, and time-resolved autofluorescence spectroscopy allowed the evaluation of tissue properties for analysis.
2. This measurement system, based on the interactions between optics and living organs, is an evaluation methodology suitable for making diagnoses during arthroscopy. It allows the quantitative and multidirectional evaluation of the original function of the cartilage based on a variety of parameters.

ACKNOWLEDGEMENTS

This work was supported by the Takeda Science Foundation, the General Insurance Association of Japan, Mitsui Sumitomo Insurance Welfare Foundation, a High-Tech Research Center Project for Private Universities, a Grant-in-Aid for Scientific Research, a Grant of the New Energy and Industrial Technology Development Organization, and the Health Labour Science Research Grant.

REFERENCES

[1] Yoshimura, N; Muraki, S; Oka, T; Kawaguchi, H & Nakamura, K. (2007). The 51st Annual General Assembly and Scientific Meeting of the Japan College of Rheumatology, *Program 265*.

[2] Ishihara, M; Sato, M; Kaneshiro, N; Mitani, G; Nagai, T; Kutsuna, T & Mochida, J. (2007). Usefulness and limitation of measurement methods for evaluation of tissue-engineered cartilage function and characterization using nanosecond pulsed laser. *Proceedings of SPIE 6439*: 643909.

[3] Ishihara, M; Sato, M; Kutsuna, T; Ishihara, M; Mochida, J & Kikuchi, M. (2008). Modification of measurement methods for evaluation of tissue-engineered cartilage function and biochemical properties using nanosecond pulsed laser. *Proceedings of SPIE 6858*: 685805.

[4] Ishihara, M; Sato, M; Ishihara, M; Mochida, J & Kikuchi, M. (2006). Multifunctional evaluation of tissue engineered cartilage using nano-pulsed light for validation of regenerative medicine. In: Kim SI and Suh TS, editors. *IFMBE Proceedings, World Congress on Medical Physics and Biomedical Engineering 14*; COEX Seoul, Korea. Springer: Berlin Heidelberg. p. 3187–9.

[5] Ishihara, M; Sato, M; Kaneshiro, N; Mitani, G; Mochida, J & Kikuchi, M. (2006).

Development of a noninvasive multifunctional measurement method using nanosecond pulsed laser for evaluation of regenerative medicine for articular cartilage. *Proceedings of SPIE 6084*: 60840V.

[6] Ishihara, M; Sato, M; Sato, S; Kikuchi, T; Mochida, J & Kikuchi, M. (2005). Usefulness of photoacoustic measurements for evaluation of biomechanical properties of tissue-engineered cartilage. *Tissue Eng.11*:1234–43.

[7] Ishihara, M; Sato, M; Sato, S; Kikuchi, T; Mitani, G; Kaneshiro, N; Kikuchi, M & Mochida, J. (2005). Usefulness of the photoacoustic measurement method for monitoring the regenerative process of full-thickness defects in articular cartilage using tissue-engineering technology. Progress in biomedical optics and imaging. *Proceedings of SPIE 5695*: 288–91.

[8] Ishihara, M; Sato, M; Mochida, J & Kikuchi, M. (2007). In: Akaike T (editor). *Regeneration Medicine 4*, Bioengineering for Regeneration Medicine. Corona Publishing Co., Ltd; p. 147–67.

[9] Ishihara, M; Sato, M; Mochida, J & Kikuchi, M. (2007). Noninvasive measurement for the evaluation and validation of regeneration medicine. *J. Biosci. Biotechnol. 85*:438–41.

[10] Ishihara, M; Sato, M; Mitani, G; Mochida, J & Kikuchi, M. (2007). Monitoring of extracellular matrix formation using nanosecond pulsed laser. *Journal of Institute of Electrical Engineers of Japan 127-C*: 2166－2170.

[11] Ishihara, M; Sato, M; Sato, S; Kikuchi, T; Fujikawa, K; Kikuchi, M. (2003). Viscoelastic characterization of biological tissue by photoacoustic measurement. *Jpn J. Appl. Phys.;42*:556–8.

[12] Han, C & Barnett, B. (1973). Measurement of the rheological properties. In: Gabelnick HL and Litt M, editors. *Rheology of Biological Systems*. Illinois: Charles C. Thomas Publisher, Ltd; p. 195–217.

[13] Ishihara, M; Sato, M; Kaneshiro, N; Mitani, G; Sato, S; Mochida, J & Kikuchi, M. (2005). Development of a photoacoustic measurement method for the evaluation of regenerative medicine and tissue engineering for articular cartilage. *J. Jpn Soc. Laser Surg. Med;26*:53–9.

[14] Ishihara, M; Sato, M; Kaneshiro, N; Mitani, G; Sato, S; Mochida, J & Kikuchi, M. (2006). Development of a diagnostic system for osteoarthritis using a photoacoustic measurement method. *Lasers Surg. Med., 38*:249–55.

[15] Sato, M; Ishihara, M; Furukawa, K; Kaneshiro, N; Nagai, T; Mitani, G; Ota, N; Kokubo M; Kikuchi, M & Mochida, J. (2008). Recent technological advancements related to articular cartilage regeneration. *Med. Biol. Eng. Comput.;46:*735–43.

[16] Kutsuna, T; Sato, M; Ishihara, M; Furukawa, K; Nagai, T; Kikuchi, M; Ushida, T & Mochida, J. (2009). Noninvasive Evaluation of Tissue Engineered Cartilage with Time-Resolved Laser-Induced Fluorescence Spectroscopy. *Tissue Eng. Part C Methods.* Jul 10. [Epub ahead of print]

PRIMARY IMMUNE SYSTEM RESPONDERS TO *NUCLEUS PULPOSUS* CELLS: EVIDENCE FOR IMMUNE RESPONSE IN DISC HERNIATION

Kunihiko Murai[1]*, Daisuke Sakai[2, 3], Yoshihiko Nakamura[3], Tomoko Nakai[3], Takashi Igarashi[1], Norimasa Seo[1], Takashi Murakami[4], Eiji Kobayashi[4], and Joji Mochida[2, 3]

[1]Department of Anesthesiology and Intensive Care Medicine, Jichi Medical University, 3311-1 Yakushiji, Shimotsuke, Tochigi, 329-0498, Japan
[2]Department of Orthopaedic Surgery, Surgical Science, Tokai University School of Medicine, 143 Shimokasuya, Isehara, Kanagawa, 259-1193, Japan
[3]Research Center for Regenerative Medicine, Tokai University School of Medicine, 143 Shimokasuya, Isehara, Kanagawa, 259-1193, Japan
[4]Division of Organ Replacement Research, Center for Molecular Medicine, Jichi Medical University, 3311-1 Yakushiji, Shimotsuke, Tochigi, 329-0498 Japan

Abstract

Although intervertebral disc herniation and associated sciatica is a common disease, its molecular pathogenesis is not well understood. Immune responses are thought to be involved. This study provides direct evidence that even non-degenerated *nucleus pulposus* (NP) cells elicit immune responses. An *in vitro* colony forming inhibition assay demonstrated the suppressive effects of autologous spleen cells on NP cells and an *in vitro* cytotoxicity assay showed the positive cytotoxic effects of natural killer (NK) cells and macrophages on NP cells. Non-degenerated rat NP tissues transplanted into wild type rats and immune-deficient mice demonstrated a significantly higher NP cell survival rate in immune-deficient mice. Immuno-histochemical staining showed the presence of macrophages and NK cells in the transplanted NP tissues. These results suggest that even non-degenerated autologous NP cells are recognized by macrophages and NK cells, which may have an immunological function in the early phase of disc herniation. These findings contribute to understanding resorption and the inflammatory reaction to disc herniation.

Keywords: *Nucleus pulposus*, immune response, macrophage, natural killer cell, intervertebral disc, autoimmunity.

*Address for correspondence:
Kunihiko Murai
Department of Anesthesiology and Intensive Care Medicine,
Jichi Medical University,
3311-1 Yakushiji, Shimotsuke, Tochigi, 329-0498, Japan
Telephone Number: +81 285 58 7383
FAX Number: +81 285 44 4108
E-mail: murai.mane@jichi.ac.jp

Introduction

Resorption of herniated *nucleus pulposus* (NP) is a clinically demonstrated phenomenon during intervertebral disc herniation. In understanding the undefined pathogenesis of intervertbral disc herniation and sciatica, clarifying the molecular events that occur in resorption of NP is important. Nachemson (1969) reported decreased pH levels within and around a herniated lumbar disc and speculated that sciatica was caused by an inflammatory reaction surrounding the nerve root. Subsequently, various inflammatory chemical factors secreted from herniated NP, including tumor necrosis factor (TNF)-α (Weiler *et al.*, 2005; Le Maitre *et al., 2007*), interleukin (IL)-1β (Le Maitre *et al., 2007*) and nitric oxide (NO) (Katsuno *et al.*, 2008), have been implicated as causes of sciatica (McCarron *et al*, 1987; Geiss *et al.*, 2007). Further, the production of matrix metalloproteinases (MMPs) has been implicated in the resorption of the herniated NP (Doita *et al.*, 2001).

Bobechko and Hirsh (1965) and Gertzbein *et al.* (1975) reported that herniated NP tissue is recognized as a foreign antigen that induces an autoimmune response producing inflammation. Later, immunohistochemical (IHC) analyses of human herniated discs revealed the presence of infiltrated T cells (Park *et al.*, 2001), macrophages (Park *et al.*, 2001; Virri *et al.*, 2001), and antigen-antibody complexes in the NP (Satoh *et al.*, 1999). An *in vitro* co-culture model of macrophages and NP cells also showed the infiltration of macrophages and a decreased wet weight of the NP (Haro *et al.*, 2000). The expression of IL-6, -8, -12, and interferon (IFN)-γ suggests Th1 lymphocyte activation (Kang *et al.*, 1996; Burke *et al.*, 2002; Park *et al.*, 2002). Geiss *et al.* placed autologous porcine NP in subcutaneous titanium chambers and observed the infiltration of activated T and B cells (Geiss *et al.*, 2007), including IL-4-producing Th2 cells and γδ T cells (Geiss *et al.*, 2008). These results indicate both innate and acquired immune responses to the NP. Other studies (Park *et al.*, 2001; Jones *et al.*, 2008), however, have reported that NP cells undergo apoptosis and are phagocytised by macrophages without an immune response. Ikeda *et al.* (1996) investigated infiltrated cells consisting of macrophages and a small number of T cells, and proposed that extruded or sequestrated disc material

has the potential to be absorbed by phagocytes. It remains unclear from these reports whether immune responses are truly involved in disc herniation, and if so, which immune cells initiate the immune response.

In order to investigate whether an immune response is involved in disc herniation, fundamental research on NP cells and the immune system is required. The purpose of this study is to clarify the immune response to autologous NP cells and to identify the specific immune cells that initiate an immune response by using *in vivo* and *in vitro* rat models to assess the survival of NP cells exposed to immune system cells.

Materials and Methods

In vitro studies

Preparation of rat-tail NP cells. Male Sprague-Dawley (SD) rats (Nihon Charles River Co., Kanagawa, Japan) aged 10-12 weeks, were used for the colony forming inhibition assay (CFI), and male Lewis rats (Nihon Charles River) aged 10-12 weeks were used for the cytotoxicity assay. Following sacrifice, NP tissues were dissected from the whole tail and digested in 0.05% trypsin-ethylene diamine tetraacetic acid (EDTA; Gibco, Grand Island, NY, USA) for 15 minutes. The digestate was washed, passed through a 100 μm mesh cell strainer, the NP cells were collected by mild centrifugation (500Gx4min). These experiments were approved by the Animal Research Committee of Tokai University (071095) and conducted according to the guidelines for animal experiments.

Preparation of spleen cells. Autologous spleen cells were used as effector cells for the CFI assay and isogenous spleen cells were used for the cytotoxicity assay. Briefly, the spleens were removed, mashed and passed through a 100 μm mesh cell strainer. Red blood cells were haemolysed using 0.8% NH_3Cl. The spleen cells were collected by mild centrifugation (500Gx4min). The spleen cells (10^7cells/ml) were then incubated in RPMI-1640 medium (Invitrogen, Grand Island, NY, USA) with 15% foetal bovine serum (FBS, Qualified FBS, Invitrogen) at 37°C for five hours with IL-2 (60 IU/ml; Imunase, Shionogi, Osaka, Japan).

Purification of T cells, natural killer (NK) cells and macrophages. For cytotoxicity assays, more than 10^8 of the spleen cells isolated from a Lewis rat were suspended in fluorescence-activated cell sorting (FACS) buffer (Facs Flow, Becton Dickinson (BD) Pharmingen, Tokyo, Japan) and incubated for 30 minutes at 4°C with saturating amounts of the following antibodies: CD3 (#550353, PE mouse anti-rat CD3, BD), CD4 (#550057 Pharmingen, APC mouse anti-rat CD4, BD), CD8 (#558824, Per CP mouse anti-rat CD8a, BD), CD161 (#550978, biotin mouse anti-rat CD161, BD). The labelled spleen cells were then separated into NK cells (CD161+), CD4+T cells (CD3+CD4+), CD8+T cells (CD3+CD8+), and macrophages (remaining CD3-) using a FACS Vantage (BD).

CFI assay. For the CFI assay, the suppressive effect of immune cells (effector cells) on colony formation by autologous NP cells (target cells) was assessed by a previously described method (Spitzer *et al.*, 1980). The NP cells isolated from SD rats (N=4) were immediately utilized for the assay procedures. NP cells ($6x10^3$) and autologous spleen cells were seeded for each E:T ratio of 0:1, 25:1, 50:1 and 100:1 in 6ml of 0.9% methylcellulose formation (MethoCult H4230 Stemcell Technologies, Vancouver, Canada) in a single tube, mixed completely, then we dispensed it by 1ml in 35mm dishes (n=4 for each E:T ratio). The dishes were incubated at 37°C in 5% CO_2 and full humidity for 14 days without medium replacement, after which the number of NP colonies was scored at least twice for each dish using a tally board on the bottom of the dishes.

Cytotoxicity assay. For the cytotoxicity assay, NP cells from Lewis rats (N=2) were monolayer cultured in RPMI-1640 medium with 15% FBS for 10 days. The cells were labeled using calcein-AM (Dojin Chemical Institute, Kumamoto, Japan) for 60 minutes at 37°C without serum, washed, and seeded into 96-well V-bottomed plates (#4914, Matrix Technologies, Hudson, NH, USA) at $1x10^4$ cells/ well. Suspensions of purified isogenous NK cells, CD4+ T cells, CD8+ T cells, or macrophage cells were then added to wells at E:T cell ratios of 0:1, 25:1, 50:1 and 100:1 in a final volume of 200 μL/well in RPMI-1640 medium without serum (n = 4 for each ratio). The plate was centrifuged, then incubated in humidified air for eight hours at 37°C. After incubation, the plates were centrifuged and 100 mL of supernatant from each well was moved to another 96 well flat-bottomed plate in the same pattern, and was measured using a fluorescent plate reader (λ_{ex}=485 nm, λ_{em}=520 nm, Beckman Coulter, Brea, CA, USA). Cytotoxic activity was determined according to a modification of the ^{3}H-uridine labelling method described by Wang *et al.* (1993). Cytotoxicity was calculated as:

$$\%\text{cytotoxicity} = \frac{\text{experimental release} - \text{spontaneous release}}{\text{total release} - \text{spontaneous release}} \cdot 100 \quad (1)$$

Total release was obtained by detergent solubilisation in the presence of 1% Triton X-100 (GE Healthcare Japan, Tokyo, Japan). Spontaneous release means the fluorescence release of the pure NP cell groups. Fibroblastic cells from the *anulus fibrosus* was also analyzed as negative control.

In vivo study

For *in vivo* studies, intact rat NP tissues were transplanted with PBS into immunodeficient mice and wild type rats. The survival rate of the NP cells in the transplanted tissue was measured using the bioluminescence imaging (BLI) method described below to estimate the influence of immunity on NP cell survival. IHC staining was done on the NP tissues from the rat model to detect attracted immune cells, which would indicate the initiation of an immune response.

Transplantation of NP for the BLI study

For the BLI analysis, four male Lewis rats 10-12 weeks of

age were used as recipients of NP tissues for the Lewis to Lewis (Lew-Lew) group and four male 10-12-week-old NOD/Shi-*scid* mice (Nihon Charles River) served as recipients of NP tissues for the Lewis to NOD (Lew-NOD) group. Transgenic (Tg) male Lewis rats (8-10 weeks of age) whose tissues express luciferase produced by repeated crossing of Tg rats and confirmed in the *Organ Replacement Research Department in Jichi Medical University* were used as NP tissue donors. 100 μg of NP tissues were injected with 100 μL of PBS under the abdominal skin of recipients under general anaesthesia using 2-3% isoflurane. One donor was used for each recipient. The BLI study was conducted using a IVIS system (Xenogen Corp., Hopkinton, MA, USA) with LivingImaging acquisition and analysis software. Briefly, animals were anesthetized with isoflurane and given 125 mg/kg D-luciferin substrate (Biosynth AG, Staad, Switzerland). The animals were then placed in a light-tight chamber for imaging with a CCD camera. The photon counts from the peak luciferase activity were recorded. Luciferase activity was measured as photons emitted/second. Imaging studies were performed immediately after transplantation and at day 7, day 14 and day 21.

IHC staining

For IHC staining, male Lewis rats (n=6) were newly used as recipients of NP tissues. The transplantation procedure was the same as for the Lew-Lew group described above and one donor was used for each recipient (n=6). Two recipients were sacrificed at 5, 10, and 40 days after transplantation. In addition, two NOD mouse in BLI study was sacrificed at 26 days after transplantation. After fixation with 10% formalin for three days, a paraffin block was made though an alcohol-xylene-paraffin graded series. Five-micron thick paraffin sections were cut sagittally from the epidermis to the peritoneal membrane across the transplantation site, deparaffinized 5-μm sections first were rehydrated through xylene and graded alcohol series. For double-staining immunofluorescence, tissue slides were incubated overnight at 4°C with a primary monoclonal antibody to keratan sulphate (KS) (#270427-1, mouse anti-KS, Associates of Cape Cod, Falmouth, MA, USA), diluted 1:100 in PBS with 1% BSA, followed by incubation in darkness at room temperature for three hours with Alexa Fluor 488-conjugated anti-mouse IgG diluted 1:200. After washing with PBS, the slides were incubated overnight at 4°C in darkness with diluted (1:100) primary antibodies for rat T cells (#550353, PE mouse anti-rat CD3, BD), macrophages (#sc-9139, rabbit anti-rat CD68, Santa Cruz Biotechnology, CA, USA), or NK cells (#550978, Biotin mouse anti-rat CD161, BD). After washing with PBS, the slides with CD68 were incubated for 60 minutes in room temperature with anti-rabbit goat Alexa 594 antibody (Invitrogen); slides with CD161 staining were incubated for one hour with streptavidin-Alexa 594 (Invitrogen). All slides were then covered with Vectashield mounting medium with DAPI (H-1500, Vector Laboratories, Burlingame, CA, USA). Sample sections of day 5, day 10 and day 40 were also stained with HE and Safranin-O.

Data Analysis

All data are given as the mean ± standard deviation (SD). The statistics were processed by Excel Stat 2006 (SSRI, Tokyo, Japan). Two-factor analysis of variance (ANOVA) was employed to analyze the *in vitro and in vivo results*. The Mann-Whitney U-test was used to compare the results of the two groups in CFI assay. When significant differences were revealed by the ANOVA, *post hoc* comparisons were done. Statistical significance was defined as $p < 0.05$.

Results

***In vitro* study**

CFI assay. Spleen cells from SD rats were used as effector cells for autologous tail NP target cells. Colony formation assays showed two types of colonies that were identified as CFU-A (adherent) and CFU-NA (non-adherent) when counting colonies. Without effector cells (E:T cell ratio of 0:1), NP cells ($1x10^3$) formed CFU-NA colonies ranging in numbers from 82-118 (94.8±18.1) and CFU-A colonies ranging from 39-60 (48.3±9.6). When effector cells were added, NP cells ($1x10^3$) with an E:T cell ratio of 25:1 yielded CFU-NA colonies ranging from 26-31 (29.0±2.2) and CFU-A colonies ranging from 22-38 (28.3±6.8), an E:T cell ratio of 50:1 resulted in CFU-NA colonies ranging from 19-26 (22.8±3.0) and CFU-A colonies ranging from 19-34 (26.8±6.6) and an E:T cell ratio of 100:1 produced CFU-NA colonies ranging from 19-25 (21.0±2.8) and CFU-A colonies ranging from 18-27 (21.0±4.2). The suppressive effect of spleen cells was apparent (Fig. 1A). CFU-NA colonies were affected stronger than CFU-A colonies (Table 1). Microscopic examinations of CFU-NA

Table 1 Percentage of the number of colonies to the control (E:T cell ratio = 0:1)

E:T cell ratio	0:1	25:1	50:1	100:1
CFU-NA (%)	100	30.6±2.3	24.0±3.2	22.2±3.0
CFU-A (%)	100	58.5±14.2	55.4±13.7	43.5±8.8
p-value		p=0.021	p=0.021	p=0.019

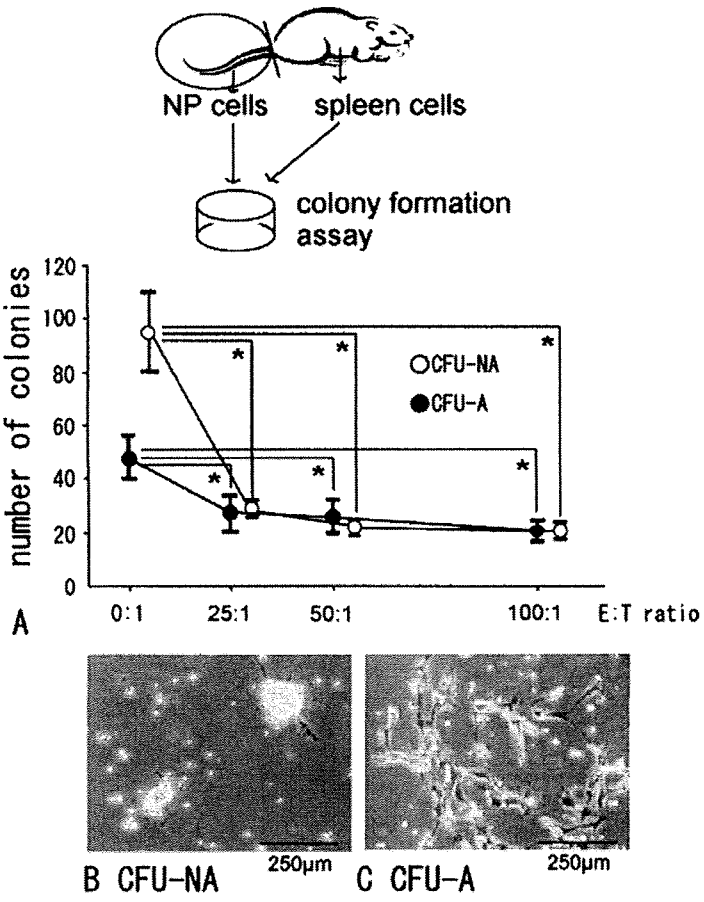

Fig. 1. (A) Results of CFI assay *in vitro*. Numbers of CFU-NA (open circle) and CFU-A (closed circle) colonies in the E: T ratio of 0:1, 25:1, 50:1 and 100:1 were counted at day 14. Colony formation of NP cells was suppressed by the addition of autologous spleen cells in both groups ($*p < 0.05$ compared with that in the E:T ratio of 0:1). (B) Attraction of spleen cells to CFU-NA. (C) Attraction of spleen cells to CFU-A. The larger number of spleen cells attracted to CFU-NA than to CFU-A supports the result in our current study that CFU-NA is more sensitive to autologous spleen cells.

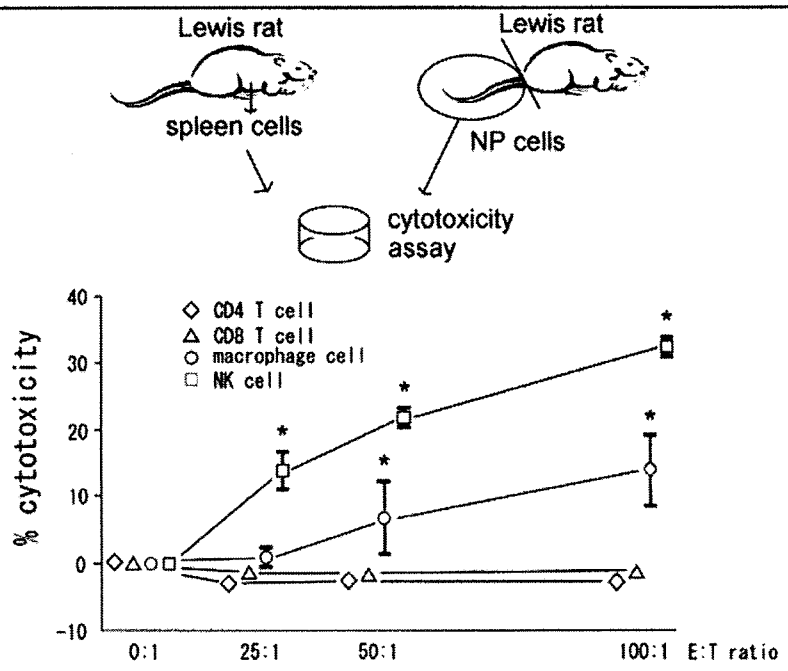

Fig. 2. Results of cytotoxicity assay *in vitro*. Cytotoxicity was calculated as follows,

$$\%\text{cytotoxicity} = \frac{\text{experimental release} - \text{spontaneous release}}{\text{total release} - \text{spontaneous release}} \times 100$$

0%=no cytotoxicity, 100%=maximum cytotoxicity as strong as detergent agent.
Cytotoxicity caused by NK cells and macrophages was suggested as a result of 8 hrs coculture ($*p < 0.05$ compared with that in the E:T ratio of 0:1).

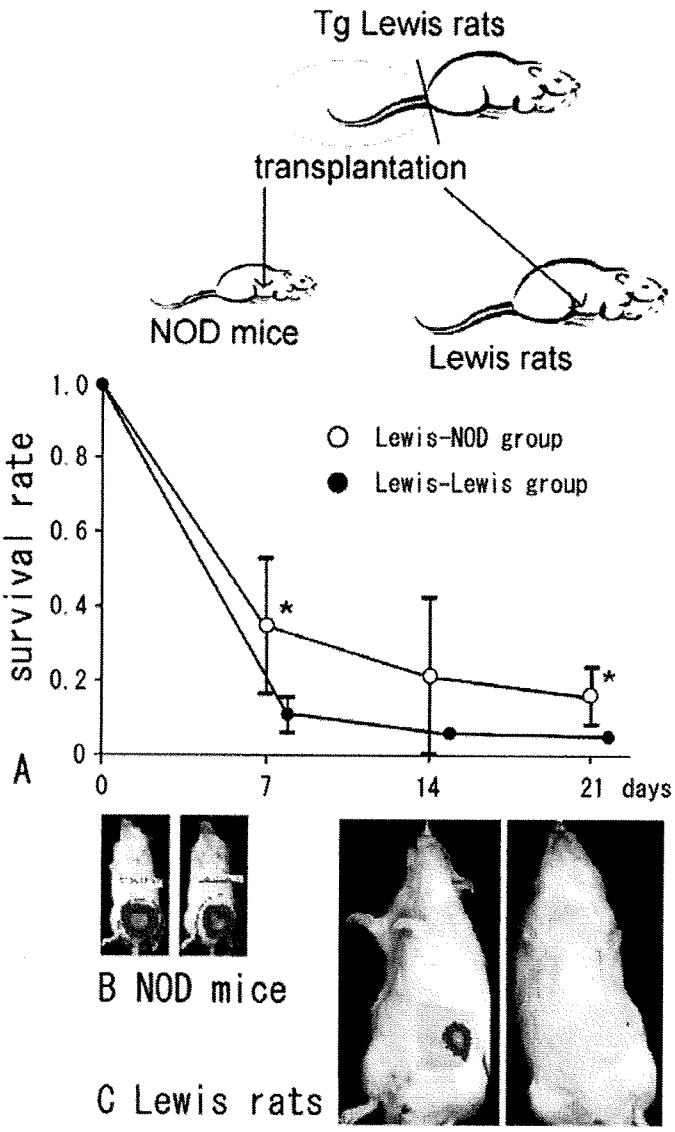

Fig. 3. (A) Survival rate of transplanted NP cells in Lewis rats and NOD mice (n=4, each). Closed circle indicates Lewis-Lewis group and open circle indicates Lewis-NOD group. Because intensity of luminescence is positively linear to the number of NP cells (data not shown), survival rate of NP cells was calculated as follows:

$$\text{Survival rate} = \frac{\text{Intensity of luminance after 7, 14 or 21 days}}{\text{Intensity of luminance just after transplantation}} \quad (2)$$

so that baseline value of survival rate (day 0) is "1". The survival rate was higher in the Lewis-NOD group than in the Lewis-Lewis group (*$p < 0.05$). (B) BLI imaging of NOD mouse at day 0 (left) and at day 90 (right). (C) BLI imaging of Lewis rat at day 0 (left) and at day 21 (right). NP cells hardly survived at day 21.

(Fig. 1B) and CFU-A (Fig. 1C) colonies revealed that larger numbers of spleen cells were attracted to CFU-NA colonies than to CFU-A colonies, further indicating that CFU-NA colony formation was more sensitive to the presence of spleen cells.

Cytotoxicity assay. From 10^8 Lewis rat spleen cells, 3.0×10^7 CD4+T cells, 2.0×10^7 CD8+T cells, 1.0×10^7 macrophages and 6.0×10^6 NK cells were sorted by FACS with data showing that more than 95% of the cells were alive.

Cytotoxicity to autologous NP cells was proportional to the E:T cell ratio in NK cells and macrophages (Fig. 2). At an E:T cell ratio of 100:1, cytotoxicity was 31-35% in NK cells and 9-20% in macrophages. Significant cytotoxicity was observed in NK cells at E:T cell ratios of 25:1 or more ($p < 0.0001$) and in macrophages at E:T cell ratios of 50:1 or more compared to the corresponding values in the absence of effector cells ($p = 0.001$ at 50:1; $p < 0.0001$ at 100:1) (Fig. 2). CD4+T cells and CD8+T cells did not have cytotoxic effects on NP cells.